

MICROMACHINING OF THICK ALUMINIUM FILMS FOR RF APPLICATIONS

* Patrick Carazzetti ¹, Marc-Alexandre Dubois ², and Nicolaas-F. de Rooij ¹

¹ Institute of Microtechnology, University of Neuchâtel, CH-2007 Neuchâtel, Switzerland

² Centre Suisse d'Electronique et de Microtechnique (CSEM SA), CH-2007 Neuchâtel, Switzerland

* Phone: +41 32 720 55 20; Fax: +41 32 720 57 11; e-mail: patrick.carazzetti@unine.ch

Abstract: Aluminium films with thicknesses up to 8 μm were sputter deposited and patterned by a highly anisotropic dry-etching process. Vertical structures exhibiting aspect ratio up to unity were demonstrated. The developed micromachining process was used for fabricating high-Q planar spiral inductors dedicated to RF applications. A peak Q-factor of 25 was obtained from a 4 nH inductor fabricated with a 3 μm -thick Al film on high-resistivity silicon. Full wave EM simulations have shown that inductors with spiral thickness up to 8 μm still allow for a significant improvement of the Q-factor in the order of 20%.

Keywords: Al dry-etching, spiral inductor, Q-factor.

INTRODUCTION

The Q-factor of the numerous inductors present in the modern RF front-end transceivers plays a fundamental role on the overall power consumption of the ever sophisticated and power-hungry portable electronic devices. A high Q-factor is of utmost importance since it contributes to reduce phase noise in oscillators, power consumption in amplifiers and insertion loss in filters. Generally, the Q-factor exhibited by on-chip inductors fabricated in standard IC technologies is drastically limited by the RF power dissipation through the low-resistivity Si substrates and by the increase of the metal resistance as a consequence of the skin and proximity effects [1,2].

In this paper we present a simple and cost-effective micromachining process enabling the fabrication of high-Q inductors based on thick Al metal spirals. We report recent developments obtained from inductively coupled plasma (ICP) etching of Al layers up to 8 μm -thick. Al was chosen as it is widely used in IC technology due to its low cost and good conductivity. The fabricated inductors on high-resistivity silicon (HRS) are suitable building-blocks for high-performance RF passive circuits, such as low-insertion loss filters and LC baluns.

FABRICATION

Figure 1 shows a SEM image of a planar inductor fabricated with a 3-mask process. Float zone single-crystal silicon wafers (Topsil Semiconductor Materials) with a measured volume resistivity of 3.5 $\text{k}\Omega\cdot\text{cm}$ were used as substrate material. First, a 3 μm -thick thermal

oxide layer was grown for providing an electrical insulation between the device and the substrate. As a second step, 200 nm of Al were sputtered and patterned by wet-etching. The underpass thus formed will connect the RF port to the centre of the spiral. This was followed by the sputtering of 1 μm -thick SiO_2 . Via-holes through this dielectric layer were then opened by dry-etching. A highly conducting top metal layer was deposited by sputtering at room temperature from a pure Al target with 2000 W DC power. The deposition rate was 6.8 nm/sec. Finally, the Al layer was patterned into spirals using a STS Multiplex ICP etching tool. The ICP source creates high-density, low-pressure and low-ion energy plasmas allowing for high etch rates and great ion directionality [3]. The combination of these characteristics enables the fabrication of high aspect ratio structures. The dry-etching process of Al was performed in a mixed Cl_2/BCl_3 plasma chemistry [4,5] at a rate of 280 nm/min. Photoresist AZ9260 spun up to 10 μm was used as mask. Examples of patterned Al spirals with thickness of 6 and 8 μm , respectively, are shown in Figure 2. In general, the anisotropic ICP etching process enabled the fabrication of vertical structures achieving aspect ratio up to unity for the whole thickness range considered, *i.e.*, from 2 to 8 μm . This performance is essential for creating a minimum spacing between adjacent tracks of an inductor, and thus maximizing the total inductance per unit area through an enhanced magnetic coupling.

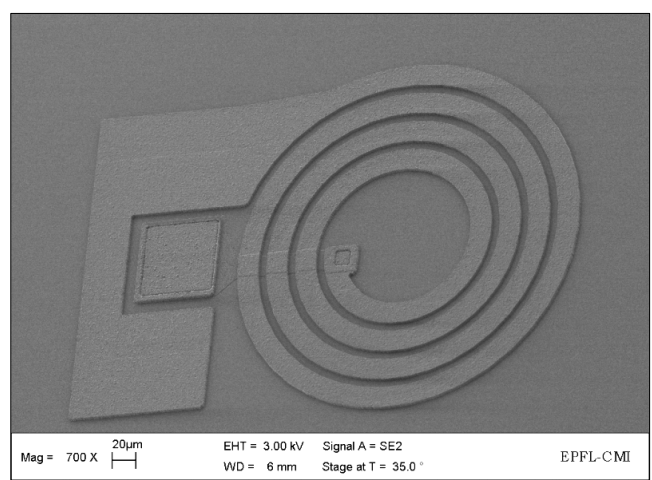


Fig. 1. SEM image of a single-port planar inductor fabricated with a 3 μm -thick Al film.

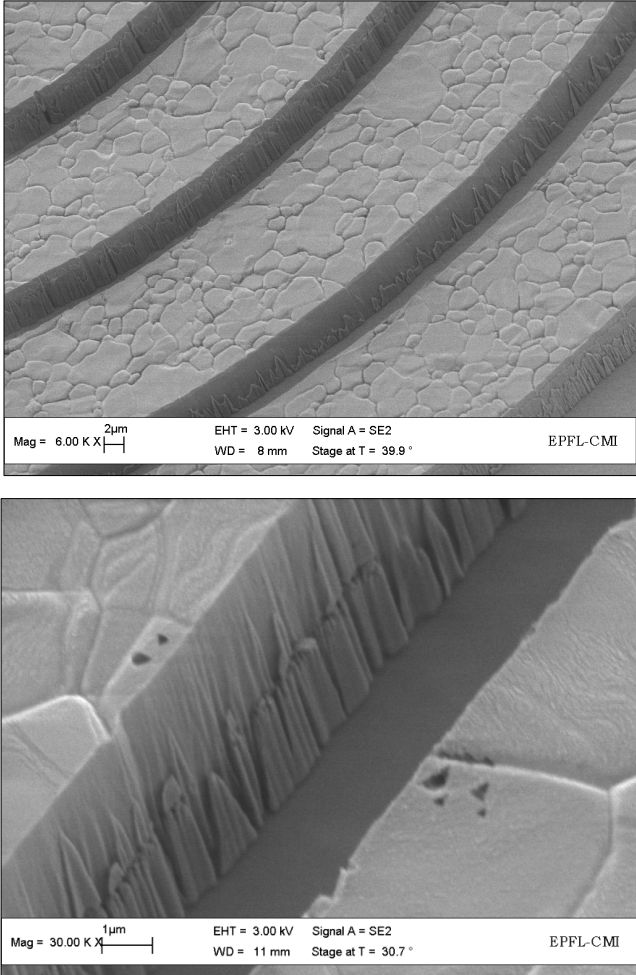


Fig. 2. SEM tilted close-up views of Al spiral inductors patterned by anisotropic ICP dry-etching process: 6 μm -thick (top) and 8 μm -thick films (bottom). In all cases the original distance separating adjacent tracks was 6 μm .

After the stripping of the residual photoresist mask no undercutting was observed and the etched areas were clear from metal residues, thus preventing the risk of short circuits during the future operation of the device. However, the patterned 6 and 8 μm -thick films presented an important wall roughness. This is a possible consequence of mask-wall deformation due to severe heating occurring during long ion bombardment processes, ultimately resulting in a non uniform pattern transfer.

The resistivity of Al films with different thickness was calculated from 4-points resistance measurements carried out on specific test structures. The trend plotted in Figure 3 highlights that films with thickness exceeding 1 μm exhibit resistivity values less than 10% away compared to the reported value for the bulk metal ($\rho_{\text{Al-bulk}} = 2.65 \cdot 10^{-8} \Omega \cdot \text{m}$). A cleaved cross section of a 5 μm -thick Al film is shown in Figure 4. Here, the cleavage procedure was performed under cryogenic conditions allowing for a brittle failure mechanism, thus preserving the original morphology formed during the sputter

deposition. The large grain size observed in the Al microstructure significantly contributes to the excellent conductivity of these films.

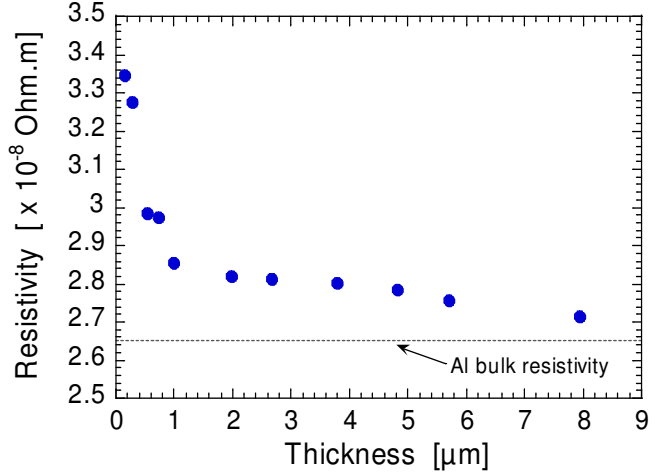


Fig. 3. Resistivity of Al films calculated from 4-points DC resistance measurements.

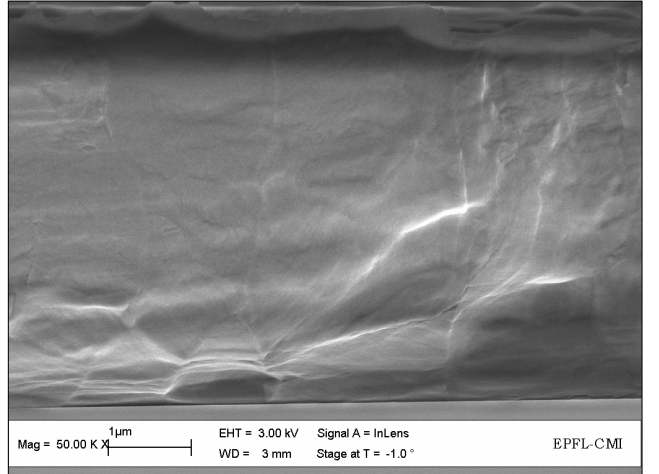


Fig. 4. SEM cross section of a 5 μm -thick Al film. The cryogenic cleavage preserved the original grain size inherent to the microstructure of the sputtered film.

RESULTS

S-parameters were measured using a HP 8510C network analyzer and Süss RF coplanar probes, and then converted to impedance. Open structures were also measured for de-embedding the inductance measurement from the parasitic capacitances associated to the probing pads. Finally, the Q-factor was calculated as the ratio of the imaginary to the real part of impedance.

Metal thickness

Figure 5 shows the impact of the spiral thickness on the device performance by comparing two inductors with

identical layout fabricated on HRS substrate with 2 or 3 μm -thick Al. The layout parameters were the following: outer diameter, $D_{out} = 400 \mu\text{m}$, track-width, $w = 20 \mu\text{m}$, interturn spacing, $s = 6 \mu\text{m}$ and 3 turns.

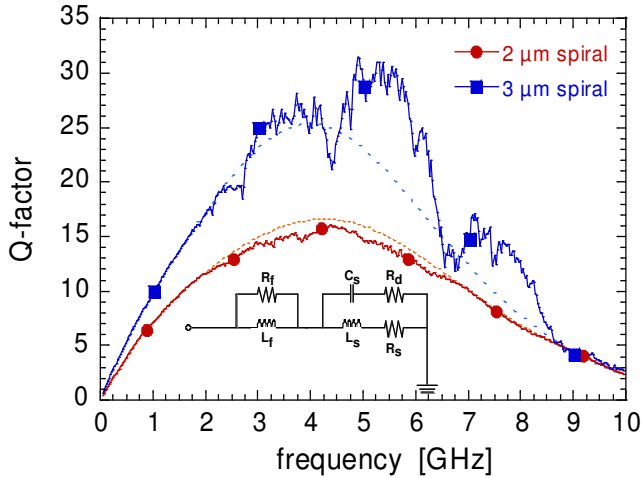


Fig. 5. Measured Q-factor (full lines) and model (dashed lines) of 3-turn inductors with identical layout, but having a different spiral thickness: 2 and 3 μm , respectively.

Figure 5 also depicts the equivalent 6-element circuit developed for modelling the inductor behaviour as a function of frequency [6]. A very accurate matching was obtained both at low and high frequency, whereas the discrepancy observed around the peak-Q region is due to the great sensitivity shown by S-parameter measurement of low resistance values. Table 1 presents the extracted low frequency values of series resistance, R_s and series inductance, L_s , as well as the obtained performances in terms of peak Q-factor and Q at 2.4 GHz displayed by 2, 3 and 4-turn inductors. As a general trend, the measured 3 μm -thick inductors, while having almost the same inductance as the corresponding set of 2 μm -thick devices exhibited peak-Q higher by 30%. Basically, the significant improvement of Q-factor is attributed to the lower resistance of thicker metal films, as confirmed by R_s values extracted from the equivalent circuit. This effect is already noticeable at low frequency, where the slope of the Q-factor curve is determined by the ratio $\omega \cdot L_s / R_s$, where ω is the angular frequency.

Table 1. Extracted series resistance, R_s , series inductance, L_s , and performances as a function of the spiral thickness.

No. of turns	Al spiral thickness [μm]	$R_s [\Omega]$	$L_s [\text{nH}]$	peak-Q @ f [GHz]	$Q_{@2.4\text{GHz}}$
2 turns	2	2.3	2.41	20 @ 5.8	12.3
3 turns	2	3.44	4.23	17 @ 4.5	13.2
4 turns	2	4.1	5.79	16 @ 3.1	13.7
2 turns	3	1.56	2.36	30 @ 5.4	18.6
3 turns	3	2.25	4.03	25.4 @ 4	19.9
4 turns	3	2.71	5.52	23 @ 3.5	19.9

Inductor geometry

Figure 6 emphasizes the role of the turn-to-turn spacing, s on the inductor characteristics by comparing a set of 3 devices with identical layout ($D_{out} = 400 \mu\text{m}$, $w = 20 \mu\text{m}$ and 3 turns), but having different distance between tracks. The extracted parameters and performances are listed in Table 2. An increase of L_s as high as 8% was observed when reducing s from 6 to 2 μm . As expected, by varying the distance between neighboring tracks of an inductor affects its inductance due to a modified mutual magnetic coupling. However, such small variation of s has shown a weaker influence on the Q-factor, meaning that the contribution of the proximity effect on the high-frequency metal resistance is negligible. In conclusion, a minimum turn-to-turn spacing allows for an increased inductance per unit area, while maintaining the same Q-factor.

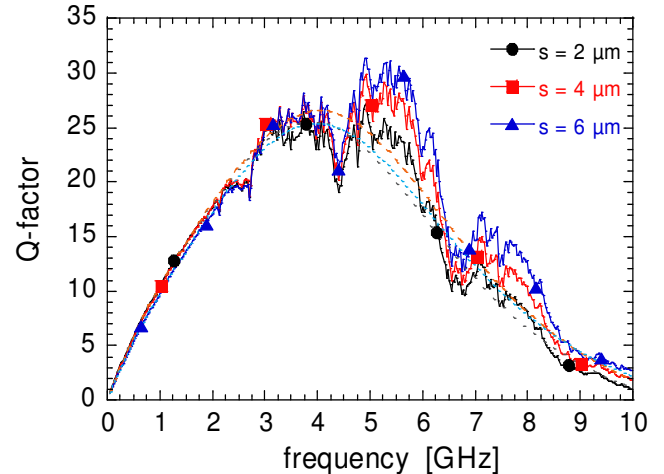


Fig. 6. Measured Q-factor (full lines) and model (dashed lines) of 3-turn inductors with identical layout, except for a different turn-to-turn spacing: 2, 4 and 6 μm , respectively.

Table 2. Extracted series resistance, R_s , series inductance, L_s and performances as a function of the turn-to-turn distance, s .

$s [\mu\text{m}]$	Al spiral thickness [μm]	$R_s [\Omega]$	$L_s [\text{nH}]$	peak-Q @ f [GHz]	$Q_{@2.4\text{GHz}}$
2	3	2.19	4.39	25.8 @ 4	20.7
4	3	2.19	4.22	26.5 @ 4	20.8
6	3	2.25	4.03	25.4 @ 4	19.9

EM simulation analysis

Figure 7 highlights the role of the spiral thickness on the inductor characteristics through results issued from full wave electromagnetic (EM) simulations performed using Sonnet® (Sonnet Software Inc., North Syracuse, NY, <http://www.sonnetusa.com>). The measured 3 μm -thick Al inductor with the following layout parameters: $D_{out} = 400 \mu\text{m}$, $w = 20 \mu\text{m}$, $s = 6 \mu\text{m}$ and 4 turns, was

considered as the reference for comparing the simulated results. Simulated data of the device with identical metal thickness have shown an excellent agreement with measurement in terms of low frequency Q-factor, L_s and self-resonance, f_{SR} (see Table 3). Based on this verification we simulated inductors with thicker coils, i.e., 6 and 8 μm . The results are plotted in Figure 7 and the obtained performances are listed in Table 3. Despite the skin-effect, which confines the flux of charges in a thin portion near the conductor surface independently of its thickness, Al films up to 8 μm still significantly reduce the conductor resistance and consequently boost the Q-factor. It is also noticed that the increase of metal thickness decreases the inductance as a consequence of the reduction of the magnetic field outside of the metal line [7]. Moreover, the increase of the spiral thickness is also accompanied by a slight increase of f_{SR} . This stems from the mentioned effect of inductance decrease, L_s being conversely proportional to the self-resonance of an inductor. This further means that the parasitic fringing field capacitance remains substantially unaffected when increasing the spiral thickness from 3 to 8 μm . In other words, the capacitive coupling between neighboring tracks of an inductor occurs almost entirely through the dielectric SiO_2 and the substrate, rather than through the air region separating the metal tracks.

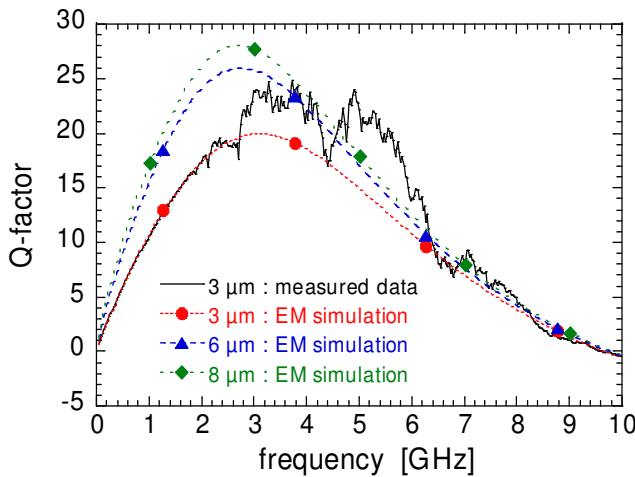


Fig. 7. Measured Q-factor (full line) of a 4-turn 3 μm -thick Al inductor compared with full wave EM simulations (dashed lines) of inductors with different spiral thickness: 3, 6 and 8 μm , respectively.

Table 3. Low frequency inductance, L_s and performances of the measured reference inductor compared with full wave EM simulations (Sonnet®).

Data source	Al spiral thickness [μm]	L_s [nH]	peak-Q @ f [GHz]	$Q_{@2.4\text{GHz}}$	f_{SR} [GHz]
Measure	3	5.52	23 @ 3.5	19.9	9.45
EM sim.	3	5.6	19.9 @ 3	18.9	9.65
EM sim.	6	5.42	26 @ 2.8	25.6	9.75
EM sim.	8	5.31	28 @ 2.7	27.7	9.83

CONCLUSION

We have presented a simple and cost-effective micromachining process for fabricating high Q-factor planar inductors dedicated to RF applications. Thick sputtered Al spirals patterned by ICP anisotropic dry-etching were the essential features of the developed process. Patterns with aspect ratio up to unity were demonstrated for film thickness up to 8 μm . A minimum interturn spacing contributes to maximize the total inductance per unit area. The measured 3 μm -thick Al spiral inductors have shown peak-Q up to 30 around 5.5 GHz for a corresponding inductance of 2.4 nH. This corresponds to a 30% improvement compared to the same inductor with a metal thickness of 2 μm . HRS substrate was chosen in order to boost the achievable Q-factor by reducing RF losses. Based on the results issued from full wave EM simulations we demonstrated that a further improvement of peak-Q up to 30% can be obtained by increasing the spiral thickness from 3 to 8 μm . Moreover, the proposed planar geometry can withstand violent mechanical shocks and vibrations and simplifies the device packaging procedure.

ACKNOWLEDGMENT

The authors would like to express their gratitude to the technical staffs of IMT-Comlab and EPFL-CMI clean room facilities for assistance and helpful discussions.

REFERENCES

- [1] W. B. Kuhn, N. M. Ibrahim, Analysis of current crowding effects on multiturn spiral inductors, *IEEE Trans. Microwave Theory & Tech.*, vol. 49, no. 1, pp. 31-38, 2000.
- [2] J. Craninckx, M. Stayaert, A 1.8-GHz low-phase-noise CMOS VCO using optimized hollow spiral inductors, *IEEE J. Solid-State Circuits*, vol. 32, no. 5, pp. 736-744, 1997.
- [3] M. Madou, *Fundamentals of Microfabrication*, CRC, Boca Raton, FL, pp. 71-79, 1997.
- [4] J. W. Lutze, A. H. Perera, J. P. Krusius, Anisotropic reactive ion etching of aluminum using Cl_2 , BCl_3 and CH_4 gases, *J. Electrochem. Soc.*, vol. 137, no. 1, pp. 249-252, 2000.
- [5] L. Colombo, F. Illuzzi, Plasma etching of aluminum alloys for submicron technologies, *Solid-State Technology*, pp. 95-100, 1990.
- [6] P. Carazzetti, M.-A. Dubois, N. F. de Rooij, High-performance micromachined RF planar inductors, *Dig. of Tech. Papers Transducers'05 – The 13th International Conference on Solid-State Sensors, Actuators and Microsystems*, Seoul, Korea, June 5-9, vol. 1, pp. 1084-1087, 2005.
- [7] Y.-S. Choi, J.-B. Yoon, Experimental analysis of the effect of metal thickness on the quality factor in integrated spiral inductors for RF IC's, *IEEE Electron Device Lett.*, vol. 25, no. 2, pp. 76-79, 2000.